Journal of Computers Vol. 33 No. 4, August 2022, pp. 215-223
doi: 10.53106/199115992022083304018

Visualization of Rotating Machinery Noise Based on Near Field Acoustic Holography

Xiao-Xia Guo[1*], Rui-Qi Zhang[1], Shu-Hao Liu[1], Chen Wan[1], Zhen-Yu Wang[1], Rong-Rong Han[2]

[1] College of Measurement and Communication Engineering, Harbin University of Science and Technology, Harbin, 150080, China
guoxiaoxia@hrbust.edu.cn
[2] Department of Civil Engineering, Harbin University, Key Laboratory of Underground Engineering Technology, Harbin, 150080, China
gongxhrr@hrbu.edu.cn

Received 1 June 2022; Revised 8 July 2022; Accepted 8 August 2022

Abstract. In order to solve the problem of fast identification of the noise source of rotating machinery, the time-space complex envelope model of monopole sound source is studied, and a modulation method of the complex envelope is proposed. A method combining near-field acoustic holography technology and complex envelope information is proposed to reconstruct the sound field and realize the identification of rotating machinery noise sources. Using the overall fluctuation of the signal to identify the noise source of the rotating machinery greatly reduces the amount of calculation, and speeds up the positioning speed while ensuring the positioning accuracy. According to the sound field radiation characteristics of rotating machinery noise, different measurement distances, different sampling points numbers and different reconstruction distances are selected to reconstruct the sound field. The simulation data analysis results show that the near-field acoustic holography technology can still obtain high sound field reconstruction accuracy under the condition of large reconstruction distance, and does not require high sampling points numbers. Using the envelope information extracted by envelope modulation technology to reconstruct the sound field can accurately identify the number and geometric distribution of sound sources. This technology not only speeds up data processing, but also ensures the accuracy of sound field reconstruction.

Keywords: near field acoustic holography, rotating machinery, spatial envelope, envelope modulation

1 Introduction

Near-field acoustic holography is an effective acoustic imaging technique proposed by J D Maynard and EG Williams et al. in the 1980s. It obtains the sound field information of unknown noise sources through hydrophones fixed on the measuring surface. The holographic algorithm was used to reverse the sound source information to realize the identification and localization of the noise source [1]. With the efforts of scholars, the near-field acoustic holography technology has developed rapidly. In 2001, J. Hald proposed the Time Domain Holography method [2]. The basic principle was to intercept the signal of a small time period in the long-time signal for analysis, and then the result was obtained. This method successfully realized the sound field reconstruction of motorcycle brake noise. In 2004, Ombeline used the near-field time-domain plane scanning method [3] and proposed four time-domain calculation methods to predict the transient sound pressure field. The parameters that affect the transient sound field reconstruction accuracy were analysed in simulation, and the sound field reconstruction accuracy of the four algorithms under different conditions was calculated. In 2009, Park and Kim used the time-domain near-field acoustic holography technology to visualize the spatial complex envelope [4-5]. Paillasseurps and Thomas validated the algorithm by using regularization methods to improve the deconvolution problem in reverse sound field reconstruction and the improved sound field reconstruction [6-9]. In 2016, Kefer introduced the robotic arm into the measurement of near-field acoustic holography, which reduced the number of microphones and accelerated the measurement speed, and studied static and dynamic near-field acoustic holography [10]. Hald proposed the wideband holography. Only a single measurement was required over a relatively short distance to obtain a single result covering the entire frequency range [11]. In 2018, S. K. Chaitanya et al. used cylindrical near-field acoustic holography (NAH) to locate the cylindrical surface sound source, and compared the direct NAH with the sound field spatial transformation (STSF). Both methods gave the correct sound source localization [12]. In 2019, Laixu Jiang proposed to use the improved Tikhonov regularization (MTR) method to solve the winding errors caused by the window function and other ill-posed problems, effectively improving the spatial resolution

* Corresponding Author

of the reconstructed sound field [13]. Dongyang Shi combined the wideband acoustic holography technology and l (1) -norm convex optimization to solve the inverse problem of sound field reconstruction. Using the advantages of the two methods, a hybrid method combining the best features of the two methods was proposed to identify the sound source location [14]. J. Antoni used an iterative method to automatically estimate the aperture function, and simultaneously completed the calculation of the aperture function and the sound source distribution [15]. In conclusion, the near-field acoustic holography technology can be applied to the identification of various types of sound sources, and all achieve high sound field reconstruction accuracy.

Large structures often contain various operating machines, equipment, power, and propulsion systems. When a working machine malfunctions, a sound space envelope may appear. The envelope information contains sound field feature information and source information. By extracting the envelope information of the signal and using it to reconstruct the sound field, the position information and geometric information of the sound source can be obtained. In order to analyse the sound source characteristics of such rotating machinery, a near-field acoustic holography technique combined with the spatial envelope of the sound field is proposed to identify and analyze the noise of rotating machinery.

2 Manuscript Preparation

According to the wave equation of small amplitude acoustic waves in an ideal fluid medium, the steady-state sound field Helmholtz equation independent of time variables can be obtained:

$$\nabla^2 p(\vec{r},\omega) + k^2 p(\vec{r},\omega) = 0 \nabla^2 p(\vec{r},\omega) + k^2 p(\vec{r},\omega) = 0 \tag{1}$$

Where: $p(\vec{r},\omega)$ is the complex sound pressure of the spatial point, $k = \omega/c = 2\pi/\lambda$ is the wave number in the fluid medium, ω is the angular frequency of the sound wave, and λ is the characteristic wavelength. First, define H as a holographic surface (measurement surface), S as a reconstruction surface (source surface), and source surface S may be any surface surrounding the sound source.

The Green's function satisfies the Dirichlet boundary condition on S, When the space of $z_H > z_S$ is a free field, the solution of any point of Eq (1) can be obtained by the Green's function formula:

$$p(x,y,z) = \int_{-\infty}^{\infty}\int_{-\infty}^{\infty} p(x_S,y_S,z_S)\cdot g_D(x-x_S,y-y_S,z-z_S)dx_S dy_S \tag{2}$$

If the sound pressure on the $z = z_S$ plane where the sound source is located is known, the sound pressure on any plane of the $z > z_S$ space can be found. Defining the relation between two-dimensional continuous Fourier transform and inverse transform in the x, y direction along the space.

$$P(k_x,k_y,z) = \int_{-\infty}^{+\infty}\int_{-\infty}^{+\infty} p(x,y,z)\, e^{-j(k_x x+k_y y)} dxdy \tag{3}$$

$$p(x,y,z) = \frac{1}{4\pi^2}\int_{-\infty}^{\infty}\int_{-\infty}^{\infty} P(k_x,k_y,z)\cdot e^{j(k_x x+k_y y)} dk_x dk_y \tag{4}$$

Where $P(k_x, k_y, z)$ is the angular spectrum of $p(x, y, z)$, and k_x, ky are the wavenumber components in the x, y direction, respectively.

After performing two-dimensional space Fourier transform on Eq (2), the convolution theorem is used to convolve the space into the product of the angular spectrum in the wavenumber domain.

$$P(k_x,k_y,z) = P(k_x,k_y,z_s)\cdot G_D(k_x,k_y,z-z_S) \tag{5}$$

In the formula, $P(k_x, k_y, z_S)$ and $G_D(kx, ky, z - z_S)$ are two-dimensional Fourier transforms of $p(x, y, z_S)$ and $g_D(x, y, z - z_x)$, respectively.

The two-dimensional space Fourier transform expression of Green's function under Dirichlet boundary condition is

$$G_D(k_x,k_y,z-z_S) = e^{jk_z(z-z_S)} \tag{6}$$

Where

$$k_z = \begin{cases} \sqrt{k^2 - k_x^2 - k_y^2} & k \geq \sqrt{k_x^2 + k_y^2} \\ i\sqrt{k_x^2 + k_y^2 - k^2} & k < \sqrt{k_x^2 + k_y^2} \end{cases} \tag{7}$$

Take the inverse Fourier transform on both sides of Eq (5) to obtain the H-plane sound pressure

$$p(x, y, z_H) = F^{-1}\left(F(p(x, y, z_S))e^{jk_z(z_H - z_S)}\right) \tag{8}$$

Where F and F^{-1} represent the Fourier transform and the inverse transform in two dimensions, respectively.

When the value of the sound pressure on $z = z_S$ is known, the sound pressure value on any plane of $z > z_S$ can be predicted. Conversely, the equation (5) by performing yields:

$$P(k_x, k_y, z_S) = P(k_x, k_y, z_H) \cdot e^{-jk_z(z_H - z_S)} \tag{9}$$

Using the above equation to obtain the sound pressure near the surface $z = z_S$ (reconstruction surface). The basic formula for planar near-field acoustic holographic reconstruction can be obtained:

$$p(x, y, z_S) = F^{-1}\left(F(p(x, y, z_H))e^{jk_z(z_H - z_S)}\right) \tag{10}$$

The far field prediction of the sound field can be completed according to Eq (8), and the near field reconstruction of the sound field amount can be realized by Eq (10).

In the reverse reconstruction of the sound field, the improved two-dimensional Harris filter window function is used to filter the noise signal in the wavenumber domain:

$$W(k_x, k_y) = \begin{cases} (k_r/k_c - 1)\left(1 - 1/2e^{(k_r/k_c - 1)/\alpha}\right), k_r \leq k_c \\ (k_r/k_c - 1)\left(1/2e^{(1 - k_r/k_c)/\alpha}\right), k_r > k_c \end{cases} \tag{11}$$

Where $k_c = 0.6\pi/\Delta$ is the cut-off wave number of the filter, Δ is the measuring distance of the measuring surface. $k_r = \sqrt{k_x^2 + k_y^2}$; α is the steepness coefficient of the window function. When α is smaller, the function value cut off steeper at k_c. Generally α is within 0.1 ~ 0.2.

3 Time-space Complex Envelope Model

In the propagation of sound, the acoustic wave characteristics are related to the wavelength ($\lambda = c/f$) in both time and space, so the time complex envelope of a narrowband signal can also cause the space complex envelope associated with it. The space complex envelope be defined in the same way as the time complex envelope is defined. Taking the monopole sound source as an example, the relationship between the space complex envelope and the time envelope is derived

Suppose a point sound source with slow amplitude changes radiates outward at the center frequency f_c, and its sound pressure $p(\vec{r}, t)$ is

$$p(\vec{r}, t) = a(\vec{r}, t)\frac{e^{-j(2\pi f_c t - k_c R + \Phi_t + \Phi_S)}}{R} \tag{12}$$

Where ϕ_t is the time phase and ϕ_s is the space phase, $k_c = 2\pi f_c/c$ is the wave number, R is the distance between the measurement point and the sound source.

Divide the amplitude in Eq (12) into two parts: one is related to the center frequency f_c, and the other is related to the slowly changing amplitude $a(r, t)$ and phase ϕ_t, ϕ_s:

$$p(\vec{r}, t) = \frac{a(\vec{r}, t)e^{-j(\Phi_t + \Phi_S)}}{R} e^{-j(2\pi f_c t - k_c R)} \tag{13}$$

The time-space complex envelope is expressible as:

$$p_{CE}(\vec{r},t) = \frac{a(\vec{r},t)e^{-j(\Phi_t+\Phi_s)}}{R} \tag{14}$$

In the above formula, $a(r, t)$ can be written as the sum of a finite number of frequency components in a narrow band:

$$a(\vec{r},t) = \sum_{n=1}^{N} c_n e^{-j(2\pi\Delta f_n t - \Delta k_n R)} \tag{15}$$

Where n is the number of frequency components in the narrow band, c_n is the coefficient corresponding to each frequency Δf_n, $\Delta f_n << f_c$, $\Delta k_n = 2\pi\Delta f_n/c$, then equation (14) can be rewritten as:

$$p_{CE}(\vec{r},t) = \sum_{n=1}^{N} c_n \frac{e^{-j(2\pi\Delta f_n t - \Delta k_n R + \Phi_t + \Phi_s)}}{R} \tag{16}$$

In Eq (16), The phase can be divided into two parts: one is the spatial complex envelope ($e^{j(\Delta k_n R - \Phi_s)}$) affected by distance; the other is the time complex envelope ($e^{-j(2\pi\Delta f_n t + \Phi_t)}$) affected by time. R contains the position information of the sound source and only affects the spatial complex envelope. So the characteristics of the spatial complex envelope are affected by the wave number and frequency of the sound source, as well as the characteristics of the sound source.

4 Modulation Method of Spatial Complex Envelope

When NAH technology is used to predict the complex envelope sound field, the convolution integral of the Fourier transform in time and space is applied at the same time, so it takes a relatively long operation time, and there is a lot of information that is redundant in practical engineering applications. For example, in the identification and location of noise sources or fault diagnosis, only the position information and geometric information of the source sound field need to be obtained, and the information is completely contained in the space envelope. So if we can extract only the spatial envelope of the target sound field, we can reduce the amount of data in the reconstruction process.

Let the initial phase be zero, and rewrite Eq (13) as a combination of frequencies:

$$p(\vec{r},t) = \sum_{n=1}^{N} c_n \frac{e^{-j(2\pi f_n t + k_n R)}}{R} \tag{17}$$

The spatial Fourier transform of the sound pressure of any frequency f_n can be written as:

$$p(x,y,z;f_n) = \frac{1}{4\pi^2}\int\int_{-\infty}^{\infty} P(k_x,k_y,z;f_n)\, e^{j(k_x x + k_y y)}\, dk_x dk_y \tag{18}$$

$p(x, y, z; f_n)$ satisfies the Helmholtz equation and is substituted into the Helmholtz equation:

$$(\nabla^2 + k^2)P(k_x,k_y,z;f_n)e^{j(k_x x + k_y y)} = 0 \tag{19}$$

For the single-frequency function $P(k_x, k_y, z; f_n)$, it is only a function of z:

$$\frac{d^2}{dz}P(k_x,k_y,z;f_n) + (k_n^2 - k_x^2 - k_y^2)P(k_x,k_y,z;f_n) = 0 \tag{20}$$

According to the norm of differential equations with constant coefficients, in the free space without reflection, the general solution of Eq (20) is expressible as:

$$P(k_x, k_y, z; f_n) = A(k_x, k_y, z; f_n) e^{jz\sqrt{k_n^2 - k_x^2 - k_y^2}} \quad \textbf{(21)}$$

The equation (19) is derived as:

$$(\nabla^2 + k_n^2) P(k_x, k_y, z; f_n) e^{j(k_x x + k_y y)} = (\nabla^2 + k_n^2) p(x, y, z; f_n) \quad \textbf{(22)}$$

Substituting Eq (18) into Eq (22) and substituting Eq (21) into Eq (19), we can obtain the expression of the wavenumber space of the sound pressure field at any frequency f_n:

$$P(k_x, k_y, z; f_n) = j\pi \frac{e^{jz\sqrt{k_n^2 - k_x^2 - k_y^2}}}{\sqrt{k_n^2 - k_x^2 - k_y^2}} e^{-j(k_x x + k_y y)} \quad \textbf{(23)}$$

The above formula is the expression of the wavenumber space of the sound source field of the point sound source with spatial complex envelope corresponding to any point frequency. By simplifying the model of $p_{CE}(\vec{r}, t)$, the relationship between the spatial complex envelope $p_{CE}(\vec{r}, t)$ and the entire sound pressure field is derived in the wavenumber space. Let the initial phase be zero; let $p_{CE}(\vec{r}, t)$ consist of only two frequency components f_m and $-f_m$, then $p_{CE}(\vec{r}, t)$ can be written as:

$$p_{CE}(\vec{r}, t) = \frac{e^{-jz(2\pi f_m t - k_m R)}}{R} + \frac{e^{-jz[2\pi(-f_m)t + (-k_m)R]}}{R} \quad \textbf{(24)}$$

The sound field $p(\vec{r}, t)$ consists of $f_1 = f_c + f_m$ and $f_2 = f_c - f_m$. The spatial two-dimensional Fourier transform of Eq (24) is expressed as

$$P_{CE}(k_x, k_y, z; f_m) = j\pi \frac{e^{jz\sqrt{k_m^2 - k_x^2 - k_y^2}}}{\sqrt{k_m^2 - k_x^2 - k_y^2}} e^{-j(k_x x + k_y y)} \quad \textbf{(25)}$$

$$P_{CE}(k_x, k_y, z; -f_m) = -j\pi \frac{e^{jz\sqrt{(-k_m)^2 - k_x^2 - k_y^2}}}{\sqrt{(-k_m)^2 - k_x^2 - k_y^2}} e^{-j(k_x x + k_y y)} \quad \textbf{(26)}$$

The two-dimensional spatial Fourier transform of the entire sound field $p(\vec{r}, t)$ is obtained by Eq (23):

$$P(k_x, k_y, z; f_1) = j\pi \frac{e^{jz\sqrt{k_1^2 - k_x^2 - k_y^2}}}{\sqrt{k_1^2 - k_x^2 - k_y^2}} e^{-j(k_x x + k_y y)} \quad \textbf{(27)}$$

$$P(k_x, k_y, z; f_2) = j\pi \frac{e^{jz\sqrt{k_2^2 - k_x^2 - k_y^2}}}{\sqrt{k_2^2 - k_x^2 - k_y^2}} e^{-j(k_x x + k_y y)} \quad \textbf{(28)}$$

The wavenumber spectrum of the spatial complex envelope and the wavenumber spectrum of the entire sound field have only different wave numbers $k_1 \rightarrow k_m$, $k_2 \rightarrow -k_m$ on the same geometric information ($e^{-j(k_x x + k_y y)}$). The frequency shift with the time complex modulation, and the wave number changes with the frequency shift. Therefore, by multiplying the Eq (27) and Eq (28) by the modulation factor M and converting them into the Eq (25) and Eq (26), a modulation method of the spatial complex envelope can be obtained.

$$M_{k_1 \rightarrow k_m}(k_x, k_y, z) = \frac{\sqrt{k_1^2 - k_x^2 - k_y^2}}{e^{jz\sqrt{k_1^2 - k_x^2 - k_y^2}}} \times \frac{e^{jz\sqrt{k_m^2 - k_x^2 - k_y^2}}}{\sqrt{k_m^2 - k_x^2 - k_y^2}} \quad \textbf{(29)}$$

$$M_{k_2 \to k_m}(k_x, k_y, z) = -\frac{\sqrt{k_2^2 - k_x^2 - k_y^2}}{e^{jz\sqrt{k_2^2 - k_x^2 - k_y^2}}} \times \frac{e^{jz\sqrt{(-k_m)^2 - k_x^2 - k_y^2}}}{\sqrt{(-k_m)^2 - k_x^2 - k_y^2}} \quad \textbf{(30)}$$

5 Simulation

A monopole source is used to simulate the sound field with a slowly varying spatial envelope oscillation sound field. Let $Lx = Ly = 4m$, $c = 1500m/s$, the three point sources with slowly changing spatial envelope oscillation be located at $(x_{s1}, y_{s1}) = (0, 1)$, $(x_{s2}, y_{s2}) = (-1, -1)$, $(x_{s3}, y_{s3}) = (1, -1)$. The center frequency of the noise source is $f_c = 2000Hz$, $\Delta fm = 20Hz$, The sound field reconstruction distance is $d_z = 0.01m$, The sound field measuring distance is $z_H = 0.02m$, the number of sampling points $N = 64$. Using near-field acoustic holography to analyze the sound field reconstruction results for the sound field with spatial complex envelope.

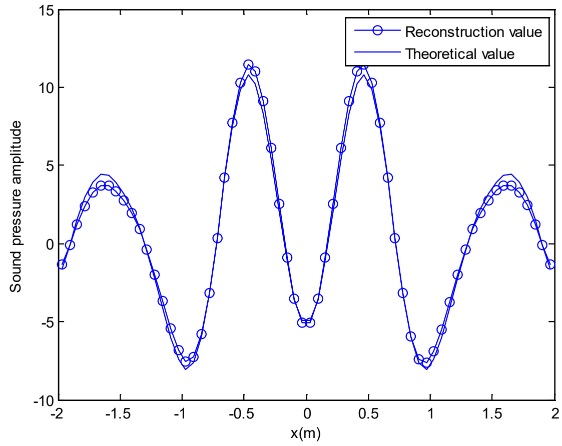

Fig. 1. The reconstructed sound field based on near-field acoustic holography

As shown in Fig. 1, when the sound field reconstruction distance $dz = 0.01m$, the sound field reconstruction sound pressure amplitude error is small, and the sound field characteristics can be accurately described. The measurement distance z_H and reconstruction distance dz are gradually increased, the sound field reconstruction accuracy of the near field acoustic hologram is further analyzed. Let $z_H = 0.1m$ and $dz = 0.05m$:

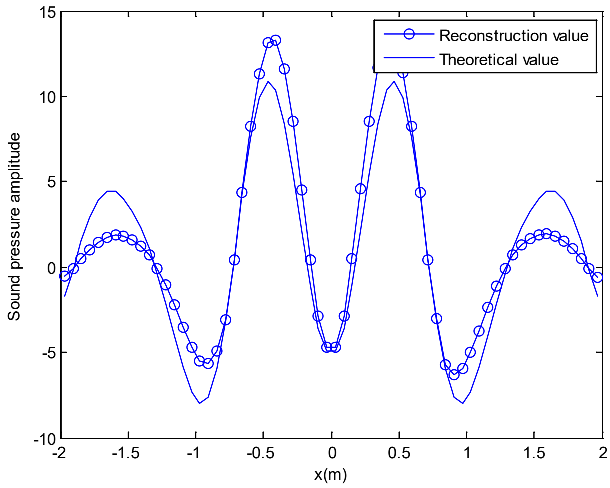

Fig. 2. The reconstructed sound field based on near-field acoustic holography

With the increase of the reconstruction distance and the measurement distance, the accuracy of the sound field reconstruction decreases from the Fig. 2, and its error is 29.35%. This result is consistent with the theory of near-field acoustic holography. The larger the measurement distance, the more representative characteristics of the sound source can be obtained. The smaller the evanescent wave component, the larger the measurement distance, the smaller the ratio of the sound source area to the measurement surface, and the larger the winding error caused by the convolution calculation, so the overall accuracy of the sound field reconstruction is reduced, but the sound field reconstruction results can reflects the characteristics of the sound source.

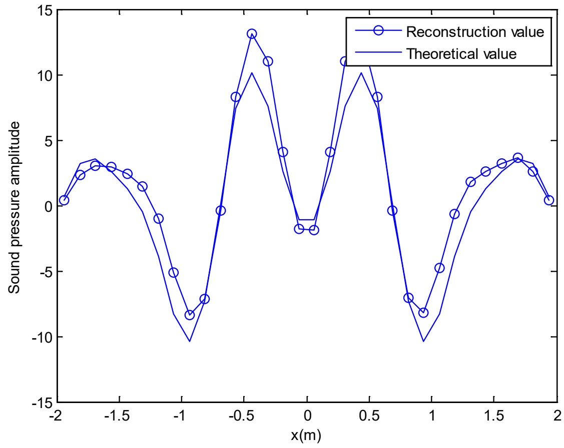

Fig. 3. The reconstructed sound field based on near-field acoustic holography

Fig. 3 shows the reconstruction results when the number of sampling points N decreases from 64 to 32 based on the near-field acoustic holographic algorithm at $z_H = 0.1m$ and $z = 0.05m$. As the number of sampling points decreases, the accuracy of the sound field reconstruction decreases, but it does not affect the judgment of the entire sound field radiation characteristics

It can be seen from the comparison of the cross-sectional diagrams that the near-field acoustic holography technology can accurately reconstruct the radiated sound field of a rotating machine using the spatial envelope information of the sound field and reflects the radiation characteristics of the sound field. However, when only the geometric information of the sound source needs to be identified and the sound source is located, the measured sound pressure value can be modulated and only the envelope information of the sound source can be extracted. The following figures (Fig. 4 and Fig. 5) show the reconstruction results before and after the sound field modulation. After modulating the sound field, the reconstruction result eliminates some redundant information, and directly gives the distribution of the sound field, and the sound source localization is accurate.

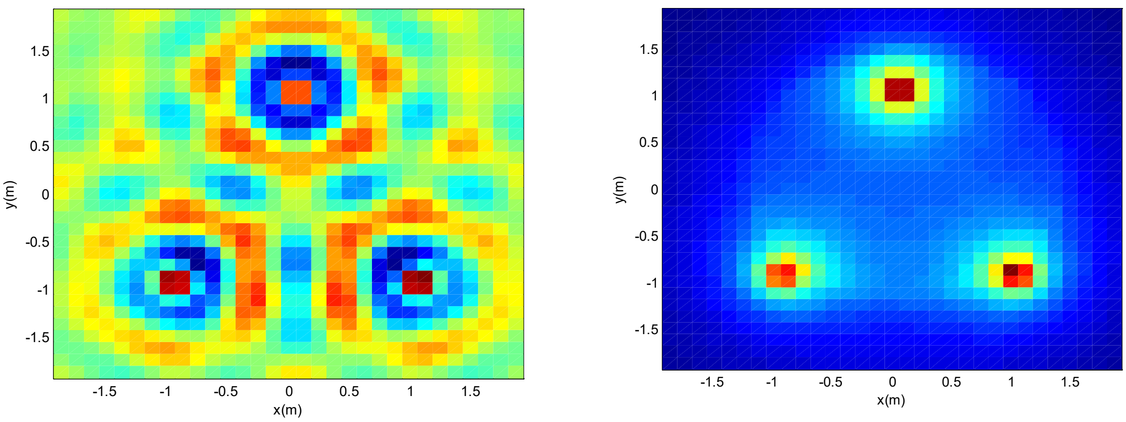

(a) Non-modulation

(b) Modulation

Fig. 4. The reconstructive results of non-modulation and modulation ($N = 32$)

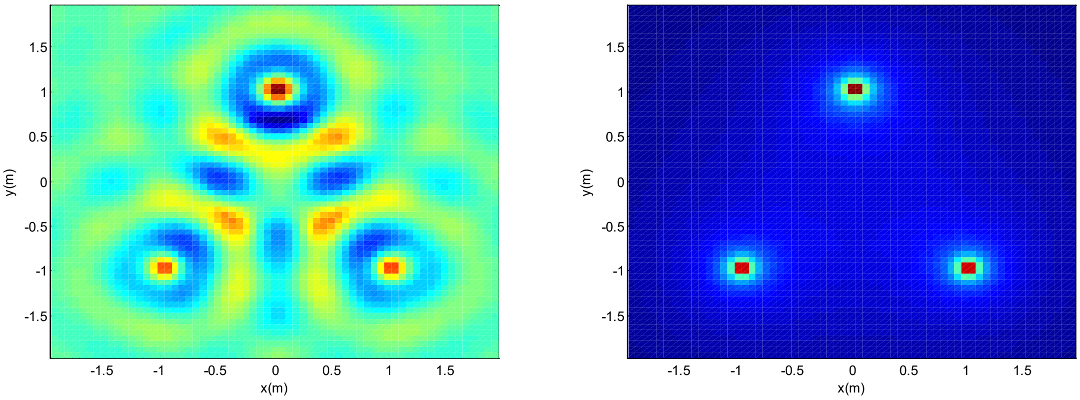

(a) Non-modulation (b) Modulation

Fig. 5. The reconstructive results of non-modulation and modulation ($N = 64$)

6 Conclusions

This paper analyses the sound field model containing the space complex envelope generated by the rotating mechanical structure, and proposes a modulation method for the space complex envelope. The near-field acoustic holography technology is used to reconstruct the sound field of the modulated sound field, so that the characteristic information of the sound source can be obtained more accurately and effectively, and the influence of redundant information on the characteristics of the sound source can be reduced. By analysing the measurement distance, the reconstruction distance and the number of sampling points, the sound field reconstruction accuracy of the near-field acoustic hologram is discussed, and the following conclusions are obtained: (1) For the radiated sound field of rotating mechanical structures, the near-field acoustic holography technology still obtains high sound field reconstruction accuracy under the condition of large reconstruction distance. It does not require more sampling points. Better reconstruction accuracy can be obtained even with fewer sampling points, so it has certain engineering application value; (2) For the sound field with envelope radiation peculiar to rotating mechanical structures, envelope modulation technology is used to extract the envelope information and perform sound field reconstruction to accurately identify the number and geometric distribution of sound sources. This technology not only accelerates the speed of data processing, but also ensures the accuracy of sound field reconstruction.

Acknowledgement

This work was supported by Joint Guidance Project of Natural Science Foundation of Heilongjiang Province (No. LH2020F033).

References

[1] J. Hald, Non-stationary STSF, Bruel & Kjær technical Review 1(2000) 1-36.
[2] J. Hald, Time domain acoustical holography and its applications, Sound and Vibration (2001) 16-25.
[3] O. Rochefoucauld, M. Melon, A. Garcia, Time domain holography: forward projection of simulated and measured sound pressure fields, The Journal of the Acoustical Society of America 116(1)(2004) 142.
[4] C.-S. Park, Y.-H. Kim, Time domain visualization using acoustic holography implemented by temporal and spatial complex envelope, The Journal of the Acoustical Society of America 126(4)(2009) 1659.
[5] C.-S. Park, Y.-H. Kim, Space domain complex envelopes: definition and a spatial modulation method, The Journal of the Acoustical Society of America 125(1)(2009) 206.
[6] V. Grulier, S. Paillasseur, J.-H. Thomas, J.-C. Pascal, Forward propagation of time evolving acoustic pressure: Formulation and investigation of the impulse response in time-wavenumber domain, The Journal of the Acoustical Society of America 126(5)(2009) 2367.
[7] J.-H. Thomas, V. Grulier, S. Paillasseur, J.-C. Pascal, Real-time near-field acoustic holography for continuously visualizing nonstationary acoustic fields, The Journal of the Acoustical Society of America 128(6)(2010) 3554.
[8] S. Paillasseur, J.-H. Thomas, J.-C. Pascal, Regularization method applied to the determination of the inverse filter of Real-time Nearfield acoustic holography, Proceedings of Inter-Noise 2009.

[9] S. Paillasseur, J.-H. Thomas, J.-C. Pascal, Regularization for improving the deconvolution in real-time near-field acoustic holography, The Journal of the Acoustical Society of America 129(6)(2011) 3777.
[10]M. Kefer, Q. Lu, Acoustic holography- A robot application, in: Proc. 2016 IEEE international conference on real-time computing and robotics (RCAR), 2016.
[11]J. Hald, Fast wideband acoustical holography, The Journal of the Acoustical Society of America 139(4)(2016) 1508.
[12]S.K. Chaitanya, S. Thomas, K. Srinivasan, Sound source localization using cylindrical Nearfield Acoustic Holography, in: Proc. INTER-NOISE and NOISE-CON Congress and Conference Proceedings, 2018.
[13]L.-X. Jiang, Y.-H. Xiao, G.-P. Zou, Data extension near-field acoustic holography based on improved regularization method for resolution enhancement, Applied Acoustic 156(2019) 128-141.
[14]T.-Y. Shi, Y.-F. Liu, J.-S. Bolton, Spatially sparse sound source localization in an under-determined system by using a hybrid compressive sensing method, The Journal of the Acoustical Society of America 146(2)(2019) 1219.
[15]J. Antoni, T. Magueresse, Q. Leclere, P. Simard, Sparse acoustical holography from iterated Bayesian focusing, Journal of Sound and Vibration 446(2019) 289-325.